NANOMATERIALS SCIENCE & ENGINEERING
Vol. 4, No. 1, pp. 5-9 (2022)

RESEARCH ARTICLE

https://doi.org/10.34624/nmse.v4i1.30015

Synthesis and characterization of multiferroic magnetoelectric ceramic composites

Indrani Coondoo

Department of Physics & CICECO-Aveiro Institute of Materials, University of Aveiro, Aveiro 3810-193, Portugal
Corresponding author, e-mail address: indrani.coondoo@ua.pt

Received 1 September 2022; accepted 16 November 2022; published online 20 December 2022

ABSTRACT

Ceramic composites with composition (1−*x*)[$Ba_{0.85}Ca_{0.15}Zr_{0.1}Ti_{0.9}O_3$] − *x*[$Ni_{0.7}Zn_{0.3}Fe_2O_4$], (0 ≤ *x* ≤ 100 wt%) were prepared using solid state route. Structural and microstructural analysis confirmed the coexistence of ferroelectric (BCZT) and magnetostrictive (NZFO) phases without any detectable presence of impurity/secondary phases. The composites exhibited ferroelectric, magnetic properties and magnetoelectric coupling responses. Highest coupling coefficient was obtained for composite with 50 wt% NZFO.

1. INTRODUCTION

Multiferroics (MFs) are those materials that exhibit, in the same phase (or multiphase), more than one primary ferroic ordering, *viz*. ferroelectricity, ferro(antiferro/ferri)magnetism, ferroelasticity or ferrotoroidicity [1]. The possibility of coupling between the ferroelectric (FE) and ferromagnetic (FM) order parameters that allows modification of polarization, *P* (magnetization, *M*) under an external magnetic field, *H* (electric field, *E*) [2], is the most intriguing aspect of MFs.

In this regard, magnetoelectric multiferroic (ME-MF) composites that combine a FE with a FM compound, have been widely studied owing to their superior coupling properties as compared with the single-phase MFs. It is the chemical '*contraindication*' between the conventional mechanism of ferroelectricity (requiring empty *d*-orbitals) and ferromagnetism (facilitated by partially filled *d*-orbitals), that limits the range of single-phase MFs. Among others, some of the prominent single-phase MF materials are: $BiFeO_3$, $BiMnO_3$, $YMnO_3$, hexagonal manganites $RMnO_3$ (where *R* represents a rare earth ion), Fe_3O_4, $Pb(Fe_{0.5}Nb_{0.5})O_3$ [3]. On the other hand, in ME-MF composites, the ferroelectric phase with large piezoelectric response and the large magnetostrictive coefficient of the magnetic phase allows strain-induced effects between the hetero-grains of the two phases generating strong ME coupling. Owing to this cross coupling, such composites, when subjected to an external *H* can tune/switch *P* (termed as *direct* ME effect; $P_i = \alpha_{ij}^E H_j$, where α_{ij}^E is the linear ME coupling coefficient) and, conversely, *M* can be modified *via* an external *E* (the *converse* ME effect; $\mu_o M_i = \alpha_{ij} E_j$, where μ_o is the magnetic permeability of vacuum) [1].

In the *direct* ME effect, the magnetoelectric voltage coefficient which is the voltage (electric field) induced in a sample by an ac magnetic field, is calculated using the relation [4]:

$$\alpha_{ij}^E = \frac{\mathrm{d}E_i}{\mathrm{d}H_j}$$

From the applications viewpoint, ME MFs can be utilized in novel devices like ultra-low power

high-density logic-memory, micro(nano) electronics, sensors, spintronics, among others [5-7].

In the present study, bulk ME-MF composites with $Ba_{0.85}Ca_{0.15}Zr_{0.1}Ti_{0.9}O_3$ (BCZT) as the piezoelectric phase and $(Ni_{0.7}Zn_{0.3})Fe_2O_4$ (NZFO) as the magnetostrictive phase were prepared and studied for their structural, microstructural and bulk properties (ferroelectric, magnetic, magnetoelectric). In the recent past, BCZT emerged as a promising lead-free compound due to its outstanding piezoelectric coefficient d_{33} ~ 600 pC/N [8], rendering BCZT as a favourable candidate for the piezoelectric phase in ME-MF composites. For the magnetostrictive phase, the spinel ferrite, $NiFe_2O_4$ (NFO), having large magnetostriction coefficient is among the most desired ferromagnetic materials. Literature survey on the relevant topic yielded no reports on composites of BCZT with the $Ni_{0.7}Zn_{0.3}Fe_2O_4$ composition and was therefore studied.

2. EXPERIMENTAL METHODS

Bulk composites of (1-*x*)$Ba_{0.85}Ca_{0.15}Zr_{0.1}Ti_{0.9}O_3$ – *x*$Ni_{0.7}Zn_{0.3}Fe_2O_4$ [BCZT-*x*NZFO; *x*=0, 10, 30, 50, 70, 90, 100 wt% or *x*=0, 0.1, 0.3, 0.5, 0.7, 0.9, 1] were fabricated using solid-state reaction method and the details can be found in ref [9]. X-ray diffraction (XRD) and field emission scanning electron microscope (FESEM) equipped with EDS (electron x-ray diffraction spectroscopy) were utilized for structural and microstructural studies. The electric field induced polarization (*P-E*) loops were acquired on a tracer based on Sawyer-Tower circuit. Magnetic measurements were performed using a vibrating sample magnetometer (VSM Lakeshore model 142A). The ME coupling coefficients were estimated from the magnetically induced voltage.

3. RESULTS AND DISCUSSIONS

The x-ray diffractograms of the powder samples of the sintered composites showed well-defined peaks corresponding to the perovskite BCZT phase and the spinel NZFO phase with no

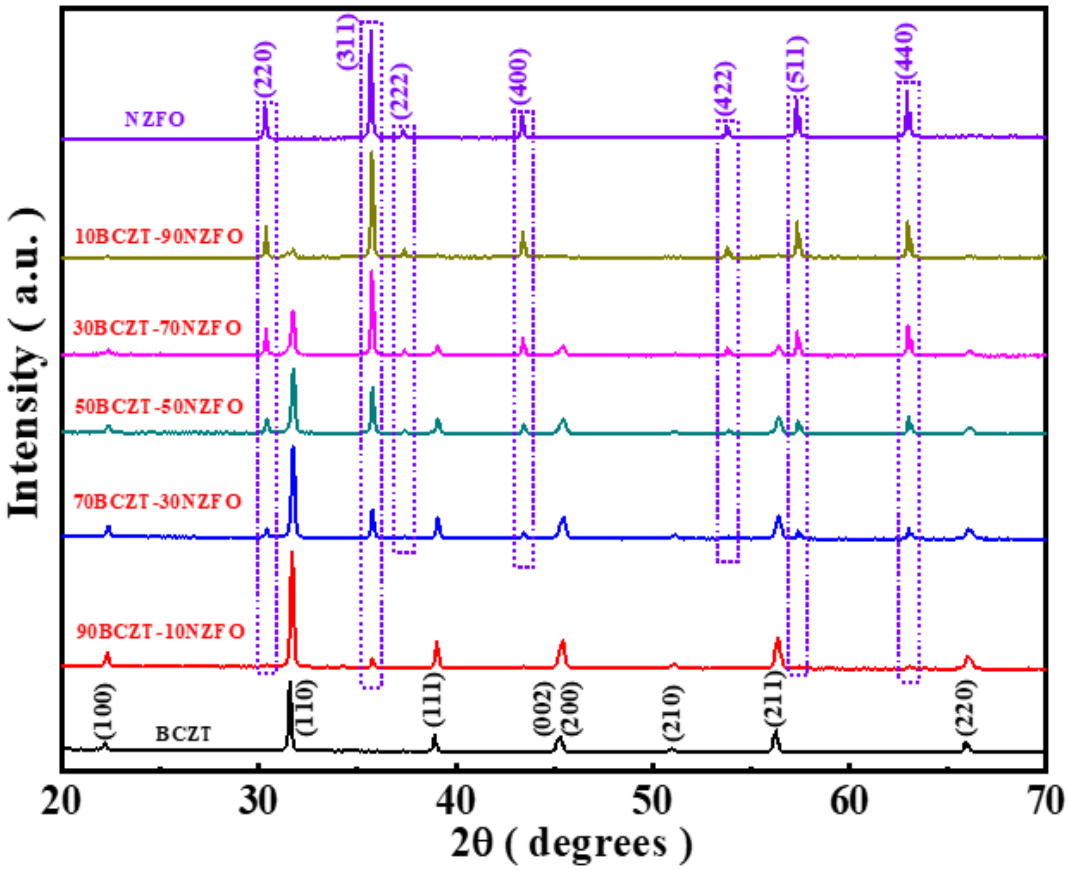

Figure 1. XRD profiles of the BCZT-*x* NZFO composites.

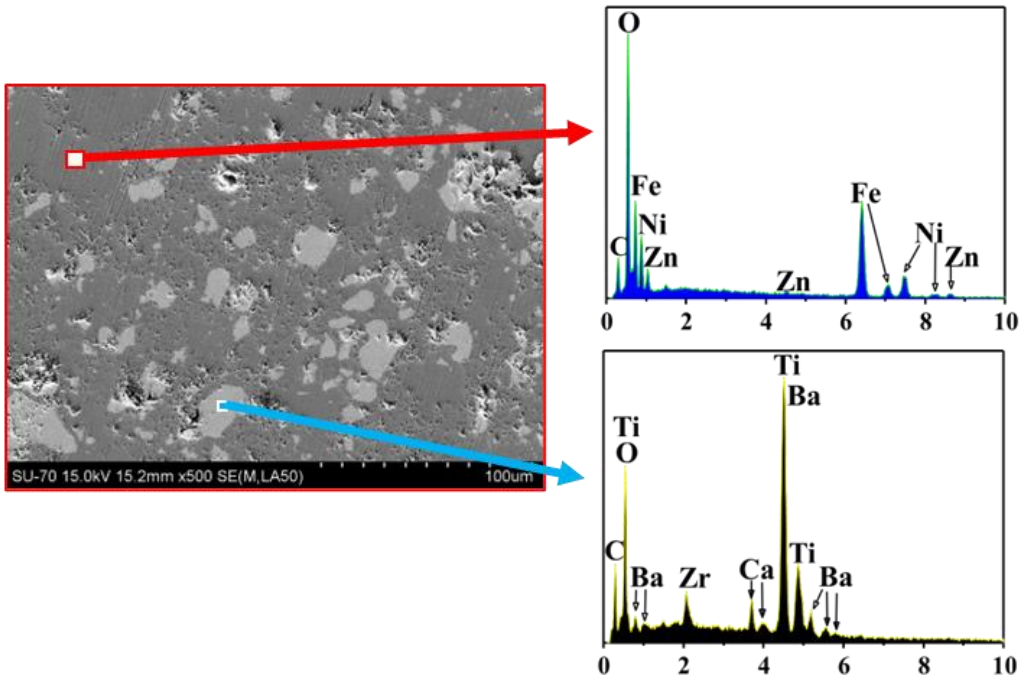

Figure 2. Backscattered electron (BSE) and EDS spectra of 50BCZT-50NZFO composite.

detectable secondary phase (Figure 1). It is observed that the peak intensity of the ferrite phase enhances with increasing content of NZFO (demarcated by dotted boxes) while those of the ferroelectric phase decrease. The density of the composites decreased from ~5.3 g/cc to 4.8 g/cc with the addition of the ferrite phase, which is attributed to the lower density of NZFO than BCZT.

The backscattered electron image of a representative sample (50BCZT-50NZFO) is shown in Fig. 2, where the lighter grains correspond to the BCZT while the darker grains belong to the NZFO phase, respectively, corroborated by the EDS spectrum shown in Fig. 2.

The polarization versus electric field (*P-E*) hysteresis loops confirmed the ferroelectric nature of the composites (Fig. 3). The saturation polarization was highest in BCZT that decreased with increasing non-ferroelectric ferrite content in the composites. The magnetization response (*M-H*) exhibited extremely slim, well-saturated hysteresis loops with very small coercivity values suggesting a long-range ferrimagnetic ordering and soft magnetic behaviour (Figure 4). The parameters from *M-H* loops: coercive field (H_c),

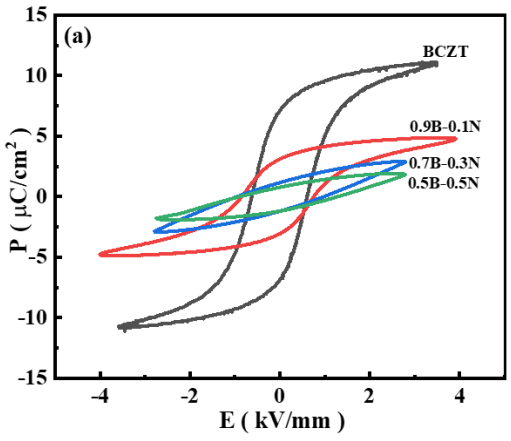

Figure 3. *P-E* hysteresis loops.

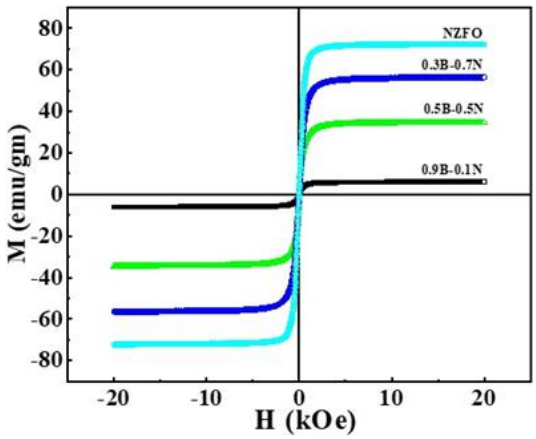

Figure 4. *M-H* hysteresis loops.

Table 1: M_s, M_r and H_c for the composites

Composition	M_S (emu/g)	M_r (emu/g)	H_c (Oe)
0.9B-0.1N	6.07	0.385	19.2
0.7B-0.3N	23.29	0.521	6.0
0.5B-0.5N	34.6	0.39	3.0
0.3B-0.7N	56.39	1.32	14.0
NZFO	72.36	2.5	20.5

saturation magnetization (M_s), and remanent magnetization (M_r), are enlisted in Table 1. As expected, the presence of the nonmagnetic BCZT phase affects the distribution of the magnetic ions and their spin orientation, and consequently a decrease in M_s and M_r is observed with increasing BCZT content in the composites. The bulk polarization and magnetization studies, thus confirm the co-existence of the individual ferroelectric and magnetic phases in the prepared composites.

In order to attest the coupling between magnetic and electric order parameters, the magnetically induced voltage (ME voltage) was measured by subjecting the samples to an *ac* magnetic field (1 Oe) at 1 kHz in the presence of a *dc* bias magnetic field, *H*. The ME coupling measurements were performed in two modes: transverse (α_{E31}) and longitudinal (α_{E33}). The coupling coefficient induced by the varying magnetic field was estimated from the relation: $\alpha_E = \partial E/\partial H \approx \frac{\delta V}{(t \cdot \delta H)}$, where δV denotes the voltage measured across the sample having thickness t. Figure 5 compares the ME coupling coefficient in 50BCZT-50NZFO composition which showed the highest α_{31} ~14.5 mV/Oe.cm and α_{33} ~12.9 mV/Oe.cm, among the studied composites. It is seen that in both the modes, the α_E trace similar magnetic field dependence: initial increase with magnetic field; thereafter reaching a maximum before gradually decreasing to nearly zero. The α_E curves should follow the piezomagnetic coefficient $q_{ik}(= \frac{d\lambda_{ik}}{dH}$, where λ_{ik} is the magnetostriction) of the magnetic phase as it changes with *H*. Initially, at lower *H*, the λ_{ik} is small and thus weak ME response is observed. However, with increasing *H*, alignment of magnetic moments along the field direction

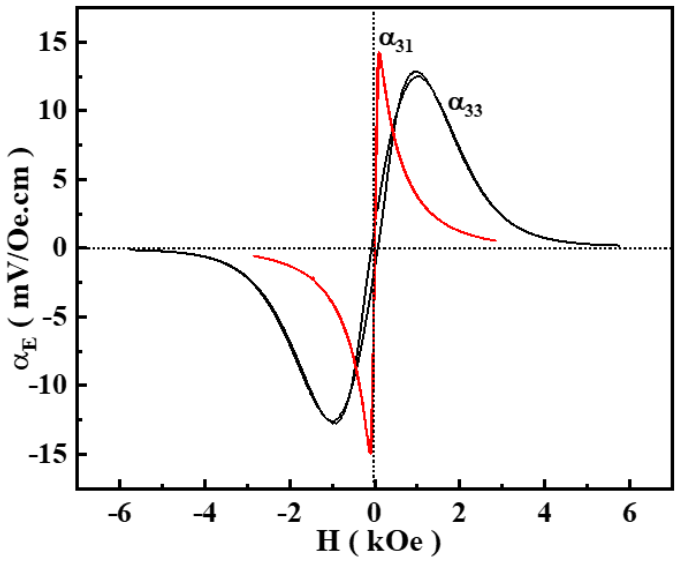

Figure 5. ME coupling coefficient in 50BCZT-50NZFO.

results in an increase in λ, thereby increasing α_E. Whereas at higher fields, λ_{ik} saturates and the piezomagnetic coefficient becomes independent of *H* and therefore α_E gradually decreases. As also noted, the transverse coupling coefficient is greater than the longitudinal coefficient, although the difference is small. This can be understood on the basis of the phase-field modelling and simulations as explained by Ma *et al.* [10]. Following their report, it is believed that in the present case, electric field poling along 3-axis causes elongation of the piezoelectric phase in the same direction (provided $d_{33} > 0$), which in turn, because of the strain-mediated elastic interaction, produces a strain in the magnetostrictive particulates along the 3-axis. This creates a magnetic domain structure having some extent of magnetization alignment along the ±3 axis, *i.e.* with a predominant 180 domain wall formation before the application of *H*. Thus, the bias magnetic field applied along 3-axis in the longitudinal mode mostly drives the 180-domain wall motion. Consequently, there is a small magnetostriction strain leading to smaller coupling coefficient (α_{33}). On the contrary, when *H* is applied in transverse geometry, a larger change in magnetostriction strain could be obtained *via* non-180-domain wall motion, resulting in higher value of α_{31}.

4. CONCLUSIONS

In conclusion, ME MF composites of (1-*x*)BCZT – *x*NZFO were successfully synthesized. The composites exhibited their individual ferroic (ferroelectric and magnetic) characteristics. Maximum ME coupling was achieved in the composite with an optimum weight fraction of 50 wt% ferrite content.

ACKNOWLEDGMENTS

I.C. would like to acknowledge financial assistance by national funds (OE), through FCT – Fundação para a Ciência e a Tecnologia, I.P., in the scope of the framework contract foreseen in the numbers 4, 5 and 6 of the article 23, of the Decree-Law 57/2016, of August 29, changed by Law 57/2017, of July 19. This work was partially developed within the scope of the project CICECO-Aveiro Institute of Materials, UIDB/50011/2020, UIDP/50011/2020 & LA/P/0006/2020, financed by national funds through the FCT/MEC (PIDDAC).

REFERENCES

[1] N.A. Spaldin and R. Ramesh, *Nat. Mater.* **18(3)**, 203-212 (2019).
[2] M.I. Bichurin, Magnetoelectric Composites. Jenny Stanford Publishing (2019).
[3] C.A.F.Vaz, J.Hoffman, C.H.Ahn, Ramamoorthy Ramesh, *Advanced Materials* **22(26-27)**, 2900-2918 (2010).
[4] M.Etier, V.V. Shvartsman, S.Salamon, Y.Gao, H. Wende, D.C.Lupascu, *Journal of the American Ceramic Society* **99**(11), 3623-3631 (2016).
[5] S. Manipatruni, D. E Nikonov, Chia-Ching Lin, T. A. Gosavi, H. Liu, B. Prasad, Y.-L.Huang, E. Bonturim, R. Ramesh, I.A.Young, *Nature* **565(7737)**, 35-42 (2019).
[6] D.K.Pradhan, A.K.Mishra, S.Kumari, A.Basu, M.Somayazulu, E.Gradauskaite, R.M. Smith, J. Gardner, P. W. Turner, A. T. N'Diaye, M. B. Holcomb, R. S. Katiyar, P.Zhou, G.Srinivasan, J. M. Gregg & J. F. Scott, *Scientific Reports* **9(1)**, 1685 (2019).
[7] S. Kumari, *et al.*, B.D. Stojanovic, Editor. 2018, Elsevier. p. 571-591.
[8] W. Liu, and X. Ren, *Physical Review Letters* **103**(25), 257602 (2009).
[9] I. Coondoo, J. Vidal, I. Bdikin, R. Surmenev, A. L. Kholkin, *Ceram. Int.* **48**, 24439 (2022).
[10] F. D. Ma, Y. M. Jin, Y. U. Wang, S. L. Kampe, S. Dong, *Aplied Physics Letters*, **104**(11), 112903 (2014).